JOURNAL OF Materials CHEMISTRY

Hydrothermal synthesis of titania photocatalyst under subcritical and supercritical water conditions

Hiromichi Hayashi* and Kazuo Torii

National Institute of Advanced Industrial Science and Technology, Supercritical Fluid Research Center, Nigatake 4-2-1, Miyagino-ku, Sendai 983-8551, Japan
E-mail: h-hayashi@aist.go.jp

Received 18th July 2002, Accepted 24th September 2002
First published as an Advance Article on the web 16th October 2001

Hydrothermal synthesis of titania powders was carried out under various subcritical and supercritical water conditions using titanium(IV) tetraisopropoxide as a starting material. Characterization of these hydrothermally synthesized titania powders by XRD, TEM, and N_2 adsorption measurements revealed that mesoporous anatase powders can be obtained by simple hydrothermal processing. The average pore size of the titania powders increased from 4 to 25 nm with an increase in the crystallite size of the titania nanoparticles that aggregate to form the mesoporous structure. Based on TG-DTA and FTIR spectra, surface hydroxyl groups decreased with the hydrothermal temperature, indicating that the condensation of Ti–OH accelerates to form a strong network of Ti–O–Ti at higher hydrothermal temperature. The hydrothermally synthesized titania powders were used for photocatalytic hydrogen evolution in an aqueous methanol suspension. Photocatalytic activity of hydrothermally synthesized titania powders was found to be much higher in comparison with some commercial titania photocatalysts. Activities per unit surface area of more than 10 were obtained for the photocatalysts synthesized under subcritical water conditions and between 39 and 68 for those synthesized under supercritical water conditions. The crystallinity is responsible for the highly photocatalytic performance of the titania powders hydrothermally synthesized under supercritical water conditions.

Introduction

Titania is one of the most studied semiconductors for photocatalytic reactions due to its low cost, ease of handling, and high resistance to photoinduced decomposition.[1–16] The photocatalytic activitiy of titania varies depending on its crystal phase, particle size, and crystallinity. Among the common crystalline forms of titania, anatase is generally recognized to be the most active phase as opposed to the rutile and brookite forms.[7,8] With regard to the particle size, smaller particles are usually better for photocatalysis due to high surface area.[17–19] However, amorphous titania having large surface area exhibits negligible photocatalytic performance. Ohtani *et al.* prepared titania powders of various amorphous-anatase compositions by heat treatment of amorphous titania in air. The photocatalytic activity of amorphous titania was negligible, increased with anatase content, and further improved by calcination of completely crystallized powder. The negligible activity of amorphous titania was attributed to recombination of photoexcited electrons and positive holes at defects located on the surface of the particles.[20,21] Accordingly, anatase powders with small particle size and high crystallinity are required to obtain the highly active titania photocatalyst.

Hydrothermal synthesis is a prospective method to obtain nanocrystalline titania particles, where polymorphism, particle size and crystallinity could be controlled by the hydrothermal conditions.[22–27] O'Regan and Grätzel synthesized nanoparticles of anatase by hydrolysis of titanium(IV) isopropoxide followed by hydrothermal treatment at 200 °C. Yin *et al.* prepared nanocrystallites of anatase and rutile titania with narrow particle-size distribution by hydrothermal processes starting from amorphous titania. Recently, Aruna *et al.* developed a new method of preparation of nanosize rutile titania by hydothermal synthesis from titanium isopropoxide. Although many reports so far have described the hydrothermal synthesis of titania powders, most of the reported hydrothermal processing of titania powders was carried out at temperatures below 250 °C. To our knowledge, Adschiri *et al.* reported the formation of anatase fine particles with a size of 20 nm from $TiCl_4$ as the precursor at 30 MPa and 400–450 °C.[28] In supercritical water, whose temperature and pressure is above its critical point (T_c = 374 °C and P_c = 22.1 MPa), solvent properties such as viscosity, diffusivity and dielectric constant can be widely changed by pressure and temperature. Supercritical water processing is a new route for obtaining homogeneous nanoparticles with high crystallinity because dehydration of hydrous metal oxide proceeds under supercritical water conditions owing to the low dielectric constant ($\varepsilon < 20$).[29–32] However, so far, there is no photocatalytic study using titania powders hydrothermally synthesized under supercritical water conditions.

In this work, a series of titania powders was synthesized under various subcritical and supercritical water conditions to determine the optimum preparation condition for highly active photocatalyst. The powders were characterized by XRD, N_2 adsorption, TEM, TG-DTA, FTIR and UV-vis reflectance spectra to examine the influence of the hydrothermal conditions on particle size, crystallinity and surface properties. As a test reaction, photocatalytic hydrogen evolution in an aqueous methanol suspension was applied to compare the activities for some commercial titania photocatalysts.

Experimental

Materials

Titanium tetraisopropoxide (Wako Pure Chemical Industries, Ltd.) was used without further purification. As references, commercial titania photocatalysts, Nihon Aerosil P25 and Ishihara Techno ST-01 were used for the photocatalysts. Both photocatalysts can be assigned to be anatase although the P25 photocatalyst contains a small quantity of rutile phase.

DOI: 10.1039/b207052a

Synthesis

The hydrothermal synthesis of titania powders was carried out using the following procedure: titanium tetraisopropoxide (20 g) was hydrolyzed with distilled water (200 cm^3) at room temperature with vigorous stirring. Then, the precipitate and the mother solution were placed into an autoclave to treat hydrothermally under autogenous pressure. Hydrothermal temperatures of 100, 200, 300 and 400 °C and heating durations of 2, 8 and 24 h were employed. The equilibrium pressures for the hydrothermal temperature at 100, 200, 300 and 400 °C were 0.2, 2.1, 6.1 and 24.0 MPa (supercritical water condition), respectively. After cooling to room temperature, the products were recovered by filtration, washed with distilled water and finally dried at 50 °C for about 24 h. The titania samples are hereinafter abbreviated as HT-*A*-*B* where *A* and *B* represent the hydrothermal temperature and heating duration, respectively.

Characterization

Powder X-ray diffraction (XRD) patterns of the as-synthesized titania samples were recorded on a Rigaku Roterflex RU-300 RAD diffractometer using CuKα radiation (35 kV and 50 mA) and a scan speed of 2° min^{-1} in 2θ. The divergent and scattering slits were set at 0.5°, and the receiving slit was 0.3°. N_2 adsorption measurements were carried out at −196 °C with an automated sorption apparatus (Micromeritics ASAP 2000). The BET surface area and pore size distribution of the samples were calculated using the BET (Brunauer–Emmett–Teller) equation and the BJH (Barrett–Joyner–Halenda) formula, respectively. Transmission electron microscopy (TEM) measurement was performed using a JEOL JEM-2000EXII electron microscope, operating at 200 kV. Thermal analysis was performed using a Rigaku Thermoflex TG-8101D thermogravimetry-differential thermal analyzer (TG-DTA) referenced with recalcined alumina at a ramping rate of 5 °C min^{-1} in static air. IR spectra of the samples in KBr matrices were measured on a Perkin-Elmer Spectrum 1000 FTIR spectrometer in the range of 4000–450 cm^{-1}. UV-visible diffuse reflectance spectra were recorded on a Hitachi-340 spectrophotometer that was equipped with an integrating sphere. Powder samples were loaded in a quartz cell and measurement was taken in a wavelength range of 200–850 nm against a standard.

Photocatalytic reaction

Photocatalytic reaction was carried out at 30 °C in a Pyrex reactor attached to an inner radiation type 400 W high-pressure mercury lamp (Riko Kagaku Ltd.). An aqueous methanol solution ($CH_3OH:H_2O = 1:4$) was introduced into the reactor to give a total volume of 500 cm^3. Methanol is a sacrificial reagent for hydrogen evolution from the aqueous methanol suspensions.[10] The catalyst (*ca.* 0.3 g) was kept in suspension by stirring continuously with a magnetic stirrer and the suspension was subsequently purged with flowing N_2 gas for 30–60 min before irradiation. The photocatalytic activity was determined by measuring hydrogen gas evolution during the irradiation of the catalyst suspensions in the aqueous methanol solution. Sampling of the gas phase was carried out every 30 min using an auto-sampler (1 cm^3) directly connected to the reactor to introduce into the gas chromatograph (GL Science; GC320, Molecular Sieve 13X column, Ar carrier, TCD).

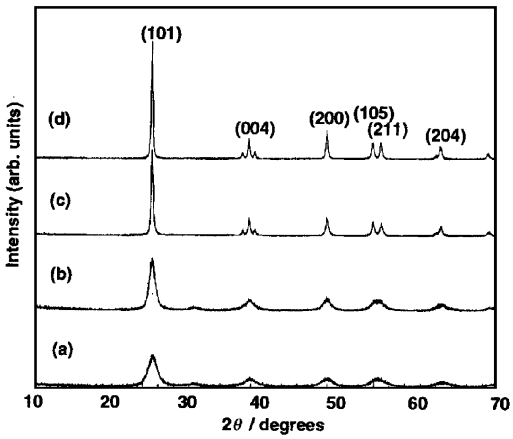

Fig. 1 Powder X-ray diffraction patterns of titania powders hydrothermally synthesized with a 24-h heating duration at 100 (a), 200 (b), 300 (c) and 400 °C (d).

Results and discussion

XRD

Fig. 1 shows XRD patterns for the titania powders hydrothermally synthesized at various temperatures. The profile for the titania powders hydrothermally synthesized can be assigned to anatase whereas a small broad signal at 31° is presumably ascribed to brookite traces in the profile for titania synthesized at 200 °C or lower. The formation of rutile is not observed , as noted by the flat background in the region of the two most intense rutile peaks (2θ = 27.5 and 36.1°) even in the XRD patterns of titania powders synthesized at 400 °C. All the XRD patterns for the hydrothermally synthesized titania powders are quite similar, though the diffraction peaks sharpened with increasing hydrothermal temperature and the heating duration,

Table 1 Results from XRD, N_2 adsorption, TG-DTA analysis and UV-reflectance spectra

Sample[a]	Crystallite size[b]/nm	Specific surface area[c]/m^2 g^{-1}	Average pore diameter[d]/nm	Wt loss (<130 °C)[e] (%)	Wt loss (130–450 °C)[e] (%)	Band gap[f]/eV
HT-100-24	19.7	182	4.3	15.7	4.2	3.1
HT-200-2	7.1	192	6.3	8.1	3.7	3.1
HT-200-8	8.9	158	7.8	5.4	2.9	3.1
HT-200-24	27.6	129	8.7	6.6	3.2	3.1
HT-300-2	10.8	130	11.2	4.7	2.5	3.1
HT-300-8	23.8	63.7	21.0	1.8	1.1	3.2
HT-300-24	92.1	41.0	20.1	1.4	1.1	3.2
HT-400-2	28.6	35.1	24.9	1.1	0.7	3.2
HT-400-8	40.1	27.0	19.8	0.7	1.0	3.2
HT-400-24	115.1	6.0	—	1.0	1.0	3.2
P25	25.0	49.0	12.1	2.0	1.2	3.2
ST-01	7.0	300.0	—	13.3	4.6	3.2

[a]Sample HT-*A*-*B* denotes hydrothermal-temperature (°C)-duration times (hours). [b]Calculated from the (101) diffraction peak of anatase using the Scherrer equation. [c]Calculated from nitrogen adsorption isotherms using the BET equation. [d]Calculated from nitrogen desorption isotherms using the BJH method. [e]Determined by thermogravimetry analysis. [f]Determined by UV-vis reflectance spectroscopy.

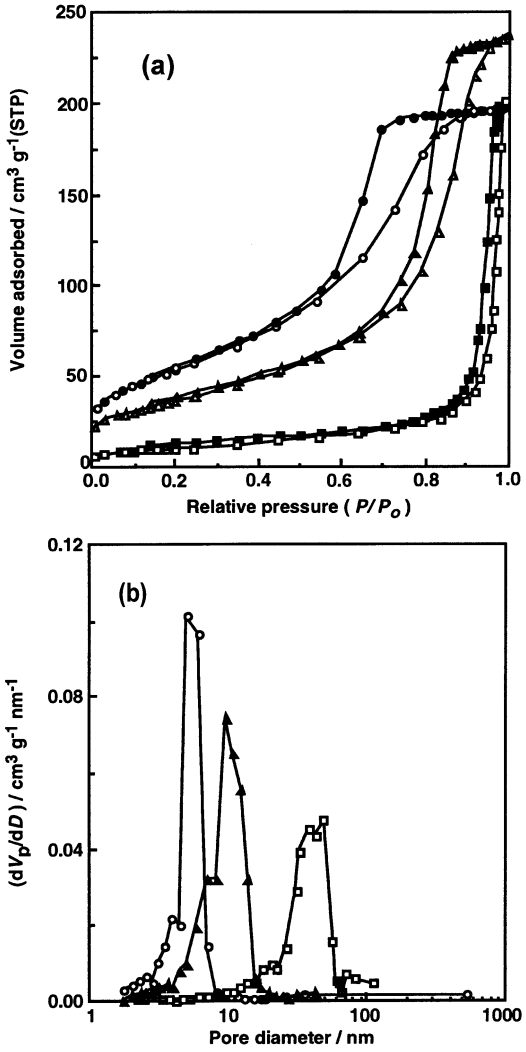

Fig. 2 (a) Nitrogen adsorption–desorption isotherms of titania powders hydrothermally synthesized with a 2-h heating duration at 200 (○, ●), 300 (□, ▲) and 400 °C (□, ■). Open and bold symbols represent adsorption and desorption, respectively. **(b)** Pore distribution of titania powders hydrothermally synthesized with a 2-h heating duration at various temperatures; (○) 200, (▲) 300, and (□) 400 °C.

indicating increasing crystallite size. The crystallite sizes calculated from the (101) reflection using the Sherrer equation are summarized in Table 1. The crystallite size increased with the hydrothermal temperature and heating duration; it especially became markedly greater for the 24-h heating duration at 300 °C or higher. The crystallite sizes of commercial titania photocatalysts, P25 and ST-01 are *ca.* 25 nm and *ca.* 7 nm, respectively. ST-01 has the smallest crystallite size among the titania powders examined.

N_2 adsorption

Fig. 2(a) shows the N_2 adsorption and desorption isotherms for the titania powders hydrothermally synthesized at various hydrothermal temperatures. According to the IUPAC classification,[33] the BET isotherms for the hydrothermally synthesized powders exhibit a type IV curve which is characteristic of mesoporous materials. The absolute value of the volume adsorbed at $0.35 < P/P_0$ and the relative pressure where the hysteresis was observed are different in the isotherms for the powders synthesized at various hydrothermal temperatures. Especially, in the isotherm for the titania powders hydrothermally synthesized at 200 °C, the onset of capillary condensation located at moderate relative pressures, and the hysteresis loop of type H2 confirmed that the mesopores were fairly regular.

Fig. 2(b) shows the pore size distribution curves determined from the desorption branches of the isotherms in Fig. 2(a). The pore size distribution, calculated using the BJH formula, showed a single peak in the mesopore range, indicating that the pore size distribution approaches monodispersity. The narrower pore size distribution was observed for the titania powders hydrothermally synthesized at lower temperature and shorter heating duration. The surface areas (BET) and average pore diameters (BJH desorption) for the titania samples are also listed in Table 1. Upon increasing the hydrothermal temperature and heating duration, the average pore size increased from 4 to 25 nm where the pore size distribution became broader and the peak shifted towards the larger pores. Based on the crystallite size for the titania powders hydrothermally synthesized with a heating duration of 2 or 8 h, the average pore diameter coincides with the crystallite size. This means that the mesoporous structure of the hydrothermally synthesized powders is presumably built up with aggregates of primary crystallites. Therefore, the average pore sizes increased with an increase in the crystallite size of titania powders. Accordingly, the pore size of the hydrothermally synthesized titania powders can be controlled to some extent by the hydrothermal conditions. However, the mesoporous structure is collapsed owing to the larger crystallites when the heating duration increases to 24 h at 300 °C or higher. Over the temperature range investigated, the specific surface area decreased with an increase in the hydrothermal temperature and heating duration from 192 to 6 $m^2\ g^{-1}$, as depicted in Table 1.

TEM

The electron micrographs also clearly show that the aggregation was much more obvious for the samples synthesized at lower hydrothermal temperature than for the samples which were prepared under supercritical water conditions. TEM images of the titania samples hydrothermally synthesized at 200 (a) and 400 °C (b) are presented in Fig. 3. It is seen that their morphology differs considerably. The sample hydrothermally synthesized at 200 °C consists of agglomerations of >50 nm in diameter. This observation was confirmed by comparing crystalline size calculated using the Sherrer equation. The X-ray peak broadening in the pattern of the sample hydrothermally treated at 200 °C indicates a primary particle size of *ca.* 8.9 nm. Titania primary particles are associated into large agglomerates.

The formation of such aggregates of nanocrystallites is a prevalent phenomenon.[34] In subcritical water, the solubility of

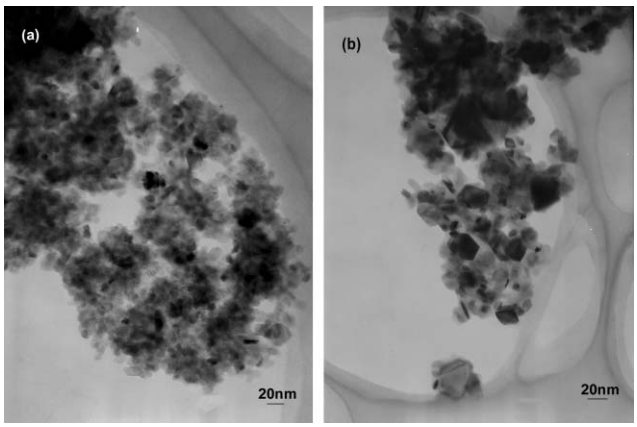

Fig. 3 Transmission electron micrographs of titania powders hydrothermally synthesized at 200 (a) and 400 °C (b) with an 8-h heating duration.

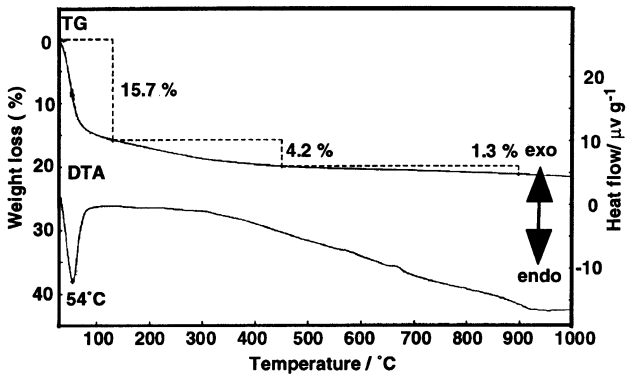

Fig. 4 TG-DTA profiles of titania powders hydrothermally synthesized at 100 °C with a 24-h heating duration.

hydrous metal oxide species can be expected to be high, during dissolving and recrystallization, primary particles aggregate to form the cloud-like products. On the other hand, it is seen that the particles of the titania powders synthesized at 400 °C are crystalline: the faces are predominantly oriented along the <101> direction. The particle size is compatible with the crystallite size (*ca.* 40 nm) estimated from the (101) peak of the XRD patterns, indicating that the particles are single crystals. Since hydrothermal reaction such as hydrolysis and dehydration proceeds faster in supercritical water than the corresponding reaction in subcritical water, highly crystalline products like single crystals can be achieved in supercritical water.

TG-DTA

Fig. 4 shows representive TG-DTA curves of titania powders hydrothermally synthesized at 100 °C with a 24-h heating duration. A characteristic endothermic peak observed around 55 °C is attributable to the dehydration of adsorbed water. No exothermic peak accompanied by weight loss was observed in the temperature range of 200–500 °C, indicating that organic compounds such as unhydrolyzed isopropoxide were absent in the resulting materials. The fact that a decrease in the sample weight was seen at elevating temperature up to 450 °C and thereafter it negligibly changed suggests that a tiny exothermic peak around 650 °C is independent of the dehydration that must be accompanied by the change in weight. This exothermic peak can be ascribed to the transformation of anatase to rutile which is supported by the X-ray diffraction pattern of the sample calcined at 700 °C. The TG curve suggests a two step process for loss of water: the desorption of adsorbed water between room temperature and 130 °C and the subsequent loss of hydroxyl groups up to 450 °C. The first and second weight losses tend to decrease with an increase in the hydrothermal temperature(Table 1), indicating that surface hydroxyl groups enable the condensation to proceed under subcritical and supercritical water conditions.

FTIR

The condensation of hydroxyl groups under subcritical and supercritical water conditions is supported by IR spectra of the titania powders. The FTIR spectra of the titania powders hydrothermally synthesized at various temperatures showed strong absorption bands at 3400 and 1630 cm^{-1} which are attributable to the stretching mode of the OH group and the deformation mode of molecular water (δ_{HOH}), respectively. The absorption of these bands decreased with an increase in the hydrothermal temperature. This result is compatible with the weight losses estimated from TG-DTA analyses. The broad band over the range of 400–700 cm^{-1}, taking in the shoulder around 830 cm^{-1}, is characteristic of well-ordered TiO_6 octahedrons.[35,36] This band becomes stronger for the titania powders hydrothermally synthesized at 300 °C or higher, suggesting that the condensation of Ti–OH accelerates to form a strong network of Ti–O–Ti under subcritical and supercritical water conditions.

UV-vis diffuse reflectance spectra

The UV-vis diffuse reflectance spectra of the titania powders hydrothermally synthesized at various hydrothermal temperatures were compared. The absorption edge of hydrothermally synthesized titania powders was observed at *ca.* 400–410 nm whereas the absorption edge was slightly shifted to shorter wavelength as the hydrothermal temperature was raised. Generally, the increase of the band gap energy increases with decreasing particle size with the effects of quantization.[37,38] However, in the present case, since the aggregation took place for titania crystallites hydrothermally synthesized at lower temperature, the spectrum does not shift to shorter wavelength, even when titania crystallite size is <10 nm. The band gaps estimated from the onset of the absorption for the titania powders are summarized in Table 1. The band gap for the hydrothermally synthesized titania powders is *ca.* 3.1–3.2 eV, which coincides with the reported values for anatase.[8,15,39]

Photocatalytic activity of titania powders

Photocatalytic activity over titania powders was examined by the hydrogen evolution from an aqueous methanol solution. The time courses of hydrogen evolution over titania powders suspended in the aqueous methanol solution are shown in Fig. 5. The hydrothermally synthesized titania powders exhibit constant hydrogen evolution without being deactivated in the present system. No change was observed on the used catalysts, as determined by XRD, indicating that the photodecomposition of water over titania is indeed a catalytic reaction. The hydrogen evolution rates calculated from the slope of the lines over the hydrothermally synthesized titania powders are summarized in Table 2 together with those of commercial titania photocatalysts, P25 and ST-01. The evolution rates for the hydrothermally synthesized titania photocatalysts are much higher than those of the commercial titania photocatalysts examined, especially the rates obtained for the titania photocatalysts hydrothermally synthesized at 300–400 °C and heating duration of 2–8 h, which were over 20 times greater than those of the commercial titania photocatalysts P25 and ST-01.

In the case of the titania powders synthesized at 200 °C, the activity increased with the heating duration whereas the surface

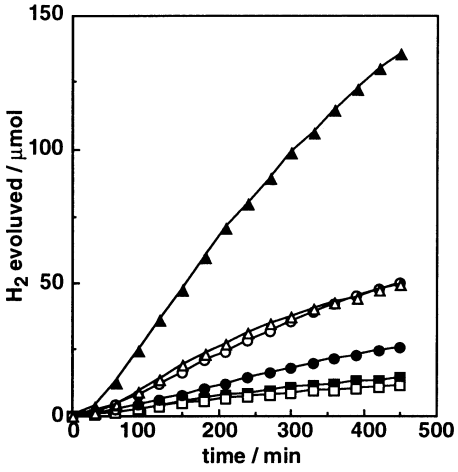

Fig. 5 Cumulative amounts of hydrogen gas evolved from an aqueous methanol solution over titania powders hydrothermally synthesized with a 24-h heating duration at 100 (●), 200 (○), 300 (▲) and 400 °C (△), P25 (■) and ST-01 (□).

Table 2 Hydrogen evolution rates of titania powders[a]

Sample	Hydrogen evolution rate	
	/μmol h^{-1} g^{-1}	/μmol h^{-1} m^{-2}
HT-100-24	123	0.68
HT-200-2	40	0.21
HT-200-8	167	1.1
HT-200-24	237	1.8
HT-300-2	1410	10.9
HT-300-8	1860	29.2
HT-300-24	640	15.6
HT-400-2	1510	43.0
HT-400-8	1830	67.9
HT-400-24	237	39.4
P25	67	1.4
ST-01	53	0.18

[a]Sample HT-*A*-*B* denotes hydrothermal-temperature (°C)-duration times (hours). Catalyst, 300 mg; solution ($MeOH:H_2O = 1:4$(v/v)), 500 cm^3; light source, high-pressure mercury lamp (400 W); reaction cell, inner irradiation reaction Pyrex cell; temperature, 30 °C.

area decreased with the heating duration. This suggests that the crystallinity of the titania powders synthesized at 200 °C is not sufficient even after long heating duration. Since there was impurity of the brookite phase in the titania powders synthesized at 200 °C or lower, as shown in the XRD results, defects were considered to exist, which might act as recombination centers for photogenerated electron-hole pairs. In contrast, the maximal activity was obtained for the titania powders synthesized at 300 or 400 °C with the 8-h heating duration. According to TEM observation, for the titania powders hydrothermally synthesized at 400 °C, the particles are crystalline. Increasing the heating duration time promotes the formation of anatase nanocrystallites with regular crystal surfaces. The anatase nanocrystals with regular crystal surfaces should have less surface defects, giving highly efficient photocatalysis by suppression of electron-hole pair recombination.[40] However, the crystallite sizes produced with the 24-h heating duration are too big for highly photocatalytic performance. In the larger and low surface area crystals, the photoexcited charges generated might have recombined in the crystals before reaching the surface of the crystals.

The photocatalytic activity per specific surface area is also summarized in Table 2. Activities per unit surface area of more than 10 were obtained for the photocatalysts synthesized under subcritical water conditions and between 39 and 68 for those synthesized under supercritical water conditions.

As mentioned above, TEM observation revealed that titania powders hydrothermally synthesized at 200 °C can be described as aggregates built of nanoparticles, while those hydrothermally synthesized at 400 °C independently exist as single crystals. When the secondary particle size becomes smaller, the more illuminated part on the grain surface is exposed to the bulk solution. This might be another reason why titania powders synthesized under supercritical water conditions exhibit highly photocatalytic performance.

Conclusions

Titania powders having mesoporosity were successfully achieved by simple hydrothermal processing. The average pore size of the resultant titania can be controlled in the size range of 4–25 nm by simply altering the hydrothermal conditions. In all cases, the main phase forming was anatase and the crystallinity of anatase increased with the hydrothermal temperature and heating duration.

The photocatalytic activities over the hydrothermally synthesized titania powders are remarkably higher than those of the commercial titania photocatalysts examined. Especially, titania powders synthesized under subcritical and supercritical water conditions exhibited higher activity than those synthesized at lower temperature. The optimal synthetic conditions for highly active titania powders can be accounted for by a suitable crystallite size with high crystallinity and less surface hydroxyl content.

In summary, this study has exhibited the advantage of hydrothermal synthesis under supercritical water conditions to prepare a highly active titania photocatalyst.

Acknowledgements

The authors wish to thank Dr Y. Onodera and Ms. T. Nagase belonging to Membrane Chemistry Lab. in our Institute (AIST) for their support on N_2 adsorption measurements and transmission electron microscopy observations.

References

1 D. Duonghong, E. Borgarello and M. Grätzel, *J. Am. Chem. Soc.*, 1981, **103**, 4685.
2 E. Borgarello, J. Kiwi, E. Pelizzetti, M. Visca and M. Grätzel, *J. Am. Chem. Soc.*, 1981, **103**, 6324.
3 K. Yamaguti and S. Sato, *J. Chem. Soc., Faraday Trans. 1*, 1985, **81**, 1237.
4 K. Sayama and H. Arakawa, *Chem. Lett.*, 1992, 253.
5 K. Sayama and H. Arakawa, *J. Chem. Soc., Chem. Commun.*, 1992, 150.
6 A. Mills and G. Porter, *J. Chem. Soc., Faraday Trans. 1*, 1982, **78**, 3659.
7 B. Kraeutler and A. J. Bard, *J. Am. Chem. Soc.*, 1978, **100**, 5985.
8 M. V. Rao, K. Rajeshwar, V. R. Pai Verneker and J. DuBow, *J. Phys. Chem.*, 1980, **84**, 1987.
9 A. Sclafani, L. Palmisano and M. Schiavello, *J. Phys. Chem.*, 1990, **94**, 829.
10 T. Kawai and T. Sakata, *J. Chem. Soc., Chem. Commun.*, 1980, 694.
11 P. Kluson, P. Kacer, T. Cajthaml and M. Kalaji, *J. Mater. Chem.*, 2001, **11**, 644.
12 A. Pottier, C. Chaueac, E. Tronc, L. Mazerolles and J.-P. Jolivet, *J. Mater. Chem.*, 2001, **11**, 1116.
13 Z. Yudn and L. Zhang, *J. Mater. Chem.*, 2001, **11**, 1265.
14 N. I. Al-Salim, S. A. Bagshaw, A. Bittar, T. Kemmitt, A. J. McQuillan, A. M. Mills and M. J. Ryan, *J. Mater. Chem.*, 2000, **10**, 2358.
15 J. A. Ayllon, A. M. Peiro, L. Saadonn, E. Vigil, X. Domenech and J. Peral, *J. Mater. Chem.*, 2000, **10**, 1911.
16 H. Kishimoto, K. Takahama, N. Hashimoto, Y. Aoi and S. Deki, *J. Mater. Chem.*, 1998, **8**, 2019.
17 Y. Suyama and A. Kato, *J. Am. Ceram. Soc.*, 1976, **56**, 146.
18 S. Nishimoto, B. Ohtani, H. Kajiwara and T. Kajiya, *J. Chem. Soc., Faraday Trans. 1*, 1985, **81**, 61.
19 A. Tsevis, N. Spanos, P. G. Koutsoukos, A. J. Linde and J. Lyklema, *J. Chem. Soc., Faraday Trans.*, 1998, **94**, 295.
20 B. Ohtani, Y. Ogawa and S. Nishimoto, *J. Phys. Chem. B*, 1997, **101**, 3146.
21 B. Ohtani, Y. Ogawa and S. Nishimoto, *J. Phys. Chem. B*, 1997, **101**, 3157.
22 B. O'Regan and M. Grätzel, *Nature*, 1991, **353**, 737.
23 C. J. Barbe, F. Arendse, P. Comte, M. Jirousek, F. Lenzmann, V. Shklover and M. Grätzel, *J. Am. Ceram. Soc.*, 1997, **80**, 3157.
24 S. D. Burnside, V. Shklover, C. Barbe, P. Comte, F. Arendse, K. Brooks and M. Grätzel, *Chem. Mater.*, 1998, **10**, 2419.
25 H. Yin, Y. Wada, T. Kitamura, S. Kambe, S. Murasawa, H. Mori, T. Sakata and S. Yanagida, *J. Mater. Chem.*, 2001, **11**, 1694.
26 H. Kominami, J. Kato, S. Murakami, Y. Kera, M. Inoue and B. Ohtani, *J. Mol. Catal. A*, 1999, **144**, 165.
27 S. T. Aruna, S. Tirosh and A. Zaban, *J. Mater. Chem.*, 2000, **10**, 2388.
28 T. Adschiri, K. Kanazawa and K. Arai, *J. Am. Ceram. Soc.*, 1992, **75**, 1019.
29 F. Cansell, B. Chevalier, A. Demourgues, J. Etourneau, C. Even, Y. Garrabos, V. Pessey, S. Petit, T. Tressaud and F. Weill, *J. Mater. Chem.*, 1999, **9**, 67.
30 R. W. Shaw, T. B. Brill, A. A. Clifford, C. A. Eckert and E. U. Franck, *Chem. Eng. News*, 1991, **69**, 26.
31 P. E. Savage, S. Gopalan, T. I. Mizan, C. J. Martino and E. E. Brock, *AIChE. J.*, 1995, **41**, 1723.

32 Z. Y. Ding, M. A. Frisch, L. Li and E. F. Gloyna, *Ind. Eng. Chem. Res.*, 1996, **35**, 3257.
33 S. J. Gregg and K. S. W. Sing, *Adsorption, Surface Area and Porosity*, Academic Press, San Diego, 1982, pp. 121–172.
34 K. Yanagisawa, Y. Yamamoto, Q. Feng and N. Yamasaki, *J. Mater. Res.*, 1998, **13**, 825.
35 V. A. Zeitler and C. A. Brown, *J. Phys. Chem.*, 1957, **61**, 1174.
36 K. A. Mautitz and C. K. Jones, *J. Appl. Polym. Sci.*, 1990, **40**, 1401.
37 R. I. Bickley, T. Gonzalez-Carreno, J. S. Lees, L. Palmisano and R. J. D. Tilley, *J. Solid State Chem.*, 1991, **92**, 178.
38 C. Kormann, D. W. Bahnemann and M. R. Hoffmann, *J. Phys. Chem.*, 1988, **92**, 5196.
39 M. Anpo, T. Shima, S. Kodama and Y. Kubokawa, *J. Phys. Chem.*, 1987, **91**, 4305.
40 M. A. Fox and M. T. Dulay, *Chem. Rev.*, 1993, **93**, 341.